2025-01-8804 Published 01 Apr 2025

Concept of an Electromechanical Brake-By-Wire System for Battery-Electric Vehicles

Marius Heydrich, Matthias Lenz, and Valentin Ivanov University of Technology Ilmenau

Julian Stoev and Johan Lecoutere Bluways International

Citation: Heydrich, M., Lenz, M., Ivanov, V., Stoev, J. et al., "Concept of an Electromechanical Brake-By-Wire System for Battery-Electric Vehicles," SAE Technical Paper 2025-01-8804, 2025, doi:10.4271/2025-01-8804.

Received: 15 Oct 2024 Revised: 20 Jan 2025 Accepted: 20 Jan 2025

Abstract

Brake-by-wire systems have received more and more attention in the recent years, but a close look on the available systems shows, that they have not reached full by-wire level yet. Most systems are still using hydraulic connections between main cylinder and the brake calipers on at least one axle to ensure functional safety. Mostly, this is the front axle, since the front brakes have to convert more kinetic energy during braking manoeuvers. Electromechanical actuators are currently used for rear brakes in hybrid brake-by-wire applications solely, since a loss of the front brake calipers can lead to severe conditions and control loss of the vehicle during braking. Further, the higher mass of battery electric vehicles (BEVs) leads to much higher braking forces on both axles and to increased sizes of the electromechanical calipers. This article presents a concept for a brake-by-wire system for battery electric vehicles, which features electromechanical brake actuators on all corners and a redundant system architecture. Theoretically, the proposed system is capable to generate a braking intensity up to 70% for vehicles with a total mass of approximately 2.8 tons. Besides mechanical design of the actuator, the power electronics are taken into account too and their behavior is investigated through dedicated simulation.

Introduction

Through the last two decades, countless driver assistant systems were released for modern vehicles to increase active safety, stability and driving comfort as well. So far, most functions are implemented with chassis components which still have a physical connection between the driver interface and the actuator, making these systems a) reliable towards functional safety and b) affordable. However, the increasing appeal for more driving assistance and automation demands for a new generation of future chassis system. There is a strong trend to fully decoupled systems, so called x-by-wire systems, that are able to adjust the driver's inputs for advanced driver assistance systems as well as automated driving functions. However, by replacing physical by electric connections, certain points about functional safety arise. Especially, in the context of safety-critical components, this conflict is very crucial, since the need to fulfill the requirement given by [1] for market release.

One of the most challenging tasks is the necessary electrification of the brake system. Traditionally, brake systems were equipped with vacuum brake boosters to limit the maximum application force [2], but already in the recent past with diesel engines in general or downsized and turbocharged gasoline engines in particular, the required vacuum was no longer available for sufficient boosting. Therefore, electric boosters were the first step to electrification, giving the possibility to further use tandem main calipers, but with option to implement new functions e.g., different pedal feedback curves for predefined driving modes. With the increasing number of hybrid and battery electric vehicles in the past and their potential of cooperative braking between the regenerative and friction brake system, rapid progressing in the brake-by-wire technology is mandatory for safe braking with a maximum amount of energy recovery. In the next section, a brief overview is given on the technical side of brake-by-wire systems. An explicit overview on the different systems, their special properties and recent development is given in the research conducted in [3, 4, 5, 6, 7, 8].

Current brake-by-wire applications still use hydraulic brake calipers due to their technical maturity, reliability and availability. Through the integration of separation valves in the brake lines, it is possible to operate completely independent from the driver, but only with the signals from an electronic control unit. In case of a loss of electric energy, the valves open and a physical connection between main cylinder and brake caliper is established as fallback level, making this type still fail-safe. Nevertheless, the full potential of brake-by-wire gets unfold through electromechanical brake (EMB) calipers.

They are completely dry, which means that no brake fluid is used and the brake pads are applied by electromechanical actuators. Further, they are characterized by higher actuation dynamics than any hydraulic or electrohydraulic brake system, and due to the accurate positioning of the pads, drag torque can be easily eliminated.

One special design is the electronic wedge brake (EWB), where the pad carrier plate is shaped as a wedge. As soon, as the pad comes into contact with the brake disc, the rotational movement of the disc is dragging the pad more into contact, leading to an amplification of the actuation force and resulting in higher clamping forces in comparison with a standard EMB. This leads to very small average power consumption values of 100 W and less [9, 10]. Hence, this innovative design with self-energized generation of the clamping force is compatible with the standard 12 V board net, which is advantageous for the use in standard ground vehicles. Even that there were still research activities on this type of EMB (see [11, 12, 13, 14, 15]), the EWB never got market-ready until today, since other EMB principles were favored. Therefore, the wedge brake is not further conducted in this research and the other EMB principles are focused. Mostly, they are realized by a brushless DC motor and a screw drive, but alternative principles are possible too e.g., the combination of linear actuators and lever mechanisms [16, 17] or cam drives [18]. A corresponding overview is given in [19]. Actual EMB actuators are just used as electronic parking brake devices in combination with a hydraulic brake caliper on the rear axle. The only use of real EMB actuators on the market is given in hybrid brake-by-wire applications as showcased by e.g., Continental or Brembo. These systems are beneficial due to the availability of components, but cannot fully support all benefits e.g., an effective blending between regenerative and friction brake torque due to the big gap in the system dynamics of electric traction machines and (electro-)hydraulic brake systems.

As mentioned, the dynamics of fully electric brakes are higher than for any (electro-)hydraulic system, so they seem to be advantageous for cooperative braking and vehicle dynamics control too, e.g. high-frequent antilock braking system, where a precise modulation of brake torque is required. Hence, the focus of many recent articles lies on the estimation [19, 20, 21, 22, 23] as well as the control of the clamping force [23, 24, 25, 26, 27, 28, 29, 30, 31, 32, 33, 34, 35, 36]. Of course, the control also needs to observe the system state to detect unintended system behavior. The missing physical link between the driver and the actuator requires fail-operational systems. Through the last years, plenty of designs, implementation, assessment and test strategies were published and further evolved, as exemplary given by [37, 38, 39, 40, 41, 42, 43].

In summary, the principle of EMB is advantageous for future ground vehicles and dynamics control, but several challenges have to be solved. Especially the impact of functional safety requirements, make the technology still not mature for broad implementation. The present article introduces a new electromechanical brake caliper for front axle applications on BEVs. It features redundant brake actuators and a redundant power supply. Besides the conception, a brief overview on some simulation results is given to show the system's feasibility. The research is outlined as follows: Section II discusses basic vehicle longitudinal dynamics, which are essential for calculation of the brake system parameters. Based on these results, Section III deals with the component design of the proposed system, while Section IV is about the experimental characterization. Section V summarized the outcomes and an outlook on future potentials is given.

Generalized Brake Dynamics

For calculation of all necessary parameters, a detailed consideration on the brake dynamics and system architecture is necessary. Since the general brake dynamics are well described in many books, the further mathematical description is limited to the most necessary points. For detailed information, refer to [44].

First, the overall braking force (F_{br}) is needed, given by the vehicle mass (m_v) and the target deceleration (a_x) by $F_{br} = m_v\, a_x$. As shown in Fig. 1, this force acts in the center of gravity (COG). The COG is a well-established simplification, where all forces on the vehicle are acting in an infinite small point. Depending on its distance to the front (l_f) and rear axle (l_r), the (static) front and rear axle loads are given as follows. The quotient l_f/l_{tot} is known as rear load ratio (ψ).

$$F_{z,r} = F_{z,tot}\frac{l_f}{l_{tot}} = m_v g \frac{l_f}{l_{tot}} \tag{1}$$

$$F_{z,f} = F_{z,tot} - F_{z,r} = F_{z,tot}\left(1 - \frac{l_f}{l_{tot}}\right) \tag{2}$$

During braking events, a specific amount of the wheel load gets shifted along the axles, so the rear axle gets lifted, while the front axle gains additional load. The total value depends of the wheelbase related height of COG (χ) as given by eq. (3) and (4). The knowledge of these dynamic wheel loads (F_z') is crucial for further steps.

FIGURE 1 Dimensions and forces of the vehicle

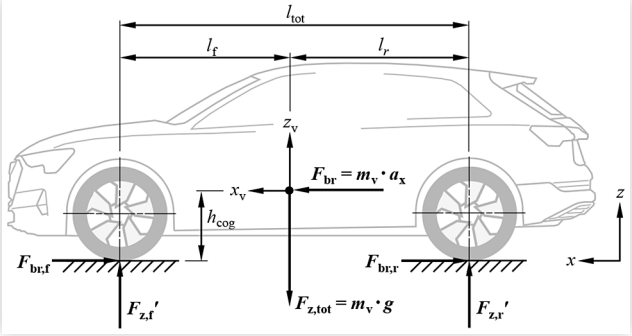

FIGURE 2 Ideal and installed brake force distributions of the target vehicle

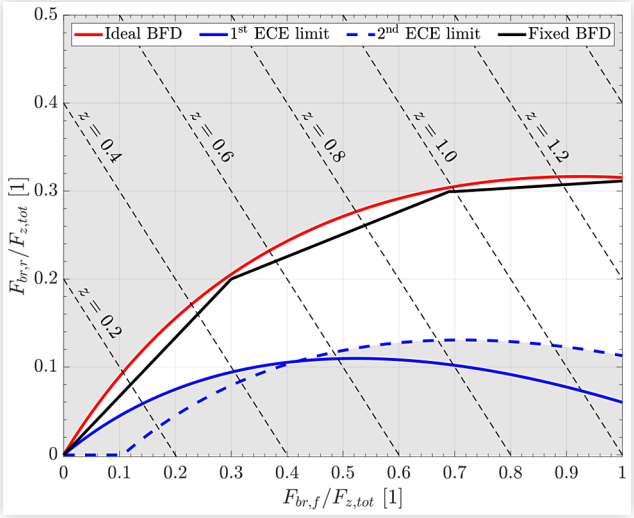

FIGURE 3 Scheme of wheel assembly containing the caliper body (①), brake pads (②) and brake disc (③), rim (④) and tire (⑤) with acting forces

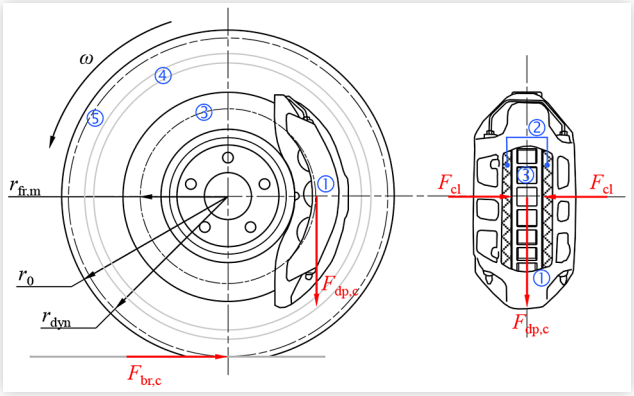

$$F_{z,f}' = F_{z,f} + m_v a_x \frac{h_{cog}}{l_{tot}} = m_v g\left(1 - \psi + \frac{a_x}{g}\chi\right) \quad (3)$$

$$F_{z,r}' = F_{z,tot} - F_{z,f}' = F_{z,r} - m_v a_x \frac{h_{cog}}{l_{tot}} = m_v g\left(\psi - \frac{a_x}{g}\chi\right) \quad (4)$$

Due to the rubber friction theory and tire dynamics from [45], the maximum longitudinal force is not only proportional to the friction force, but also to the tire patch size, so the higher the wheel load, the higher the surface pressure and therefore more braking force can be transmitted. Hence, automotive brake systems feature stronger brakes on the front axle. The brake force distribution is given by the braking intensity z (see eq. (5)).

$$z = \frac{F_{br,tot}}{F_{z,tot}} = \frac{F_{br,f}}{F_{z,tot}} + \frac{F_{br,r}}{F_{z,tot}} = \frac{\mu_f F_{z,f}'}{F_{z,tot}} + \frac{\mu_f F_{z,r}'}{F_{z,tot}} \quad (5)$$

In case, that both axles use full adhesion potential between tire and road, z equals the ratio of longitudinal and vertical tire forces, what can be replaced by the adhesion coefficient $\mu_f = \mu_r = \mu$. Reforming eq. (5) and adding eq. (3) gives an expression for the normalized braking force on the front axle.

$$\frac{F_{br,f}}{F_{z,tot}} = z\left(1 - \frac{l_f}{l_{tot}}\right) + z^2 \frac{h_{cog}}{l_{tot}} \quad (6)$$

By solving this quadratic formula and combining it with eq. (5), the ideal brake force distribution is given as follows.

$$\frac{F_{br,r}}{F_{z,tot}} = \sqrt{\left(\frac{l_r}{2h_{cog}}\right)^2 + \frac{l_{tot}}{h_{cog}}\frac{F_{br,f}}{F_{z,tot}}} - \frac{l_r}{2h_{cog}} - \frac{F_{br,f}}{F_{z,tot}} \quad (7)$$

However, it is not practicable to reach for the ideal distribution, since variations in the aforementioned parameters may lead to significant changes. Modern vehicles use the electronic brake force distribution therefore, but in the current case, a fix distribution ratio is used. The difference between both graphs is depicted in Fig. 2. Assuming an equal distribution per axle, the braking force for every corner is given by half of the total braking force per axle.

These forces are those in the tire-road contact point, but for further calculation, they must be transferred to get the friction force in the brake system. Referring to Fig. 4, the corner brake forces in the tire patch ($F_{br,c}$) and the brake disc-brake pad contact point ($F_{dp,c}$) on every corner module are proportional due to the equilibrium of wheel torques. The factor is given by the ratio of their corresponding radii, where $r_{fr,m}$ is the medium friction radius and r_{dyn} is the dynamic tire radius. Hence, the friction force is given by eq. (8), where F_{cl} is the clamping force, acting between the brake pads and the disc as soon as both get in contact and C^* is the pad coefficient. For disc brake applications, this coefficient equals two times the friction coefficient between brake pads and disc.

$$F_{dp,c} = F_{br,c}\frac{r_{dyn}}{r_{fr,m}} = F_{cl}C^* = 2F_{cl}\mu_{dp} \quad (8)$$

FIGURE 4 Clamping forces for demonstrator vehicle from Table 1

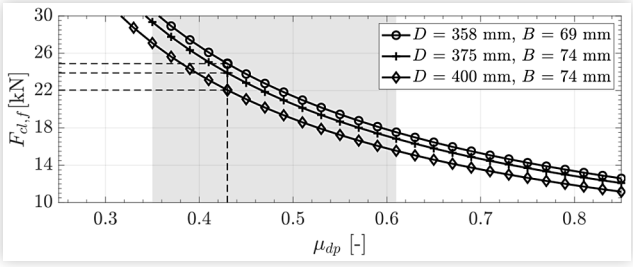

Usually, the clamping force is generated by the brake fluid, which is applied to the brake cylinders, increasing the brake pressure to the target value. In case of a full brake-by-wire system, no fluids are used. Instead, electromechanical actuators generate the clamping force. For higher reliability and to cover uncertainties in any of the parameters, a safety factor is used to ensure generation of enough braking force. Especially, the pad-disc friction underlies changes (e.g., disc corrosion, pad fatigue, temperature, ...), but referring to [46, 47, 48, 49], common values lie at μ_{dp} = 0.35 – 0.61 depending on the materials of the brake disc and brake pads. The authors of [50, 51] presented new brake pad materials and gained higher friction coefficients during experiments, but their consideration is not included in the presented study, since too high adhesion between disc and pad lead to ride discomfort.

Design of Brake-By-Wire System

This research is part of the HighScape project (https://highscape.eu), which deals with the development of innovative and scalable power electronics solutions for drivetrains, chassis actuators and auxiliary devices as well. One central point is the development of an electric brake-by-wire system. The further development is based on the project specifications as well as the technical possibilities at the time. Table 1 contains the parameters for the target vehicle. Using these values, it is possible to calculate all necessary values for the sizing of components.

Design of the Brake System Components

Since the development targets the front brakes, the calculations are limited to those only. With the data from Table 1, the braking forces are $|F_{br,f}| \approx 11$ kN. The clamping forces of every front corner can be calculated by eq. (8) including the multiplication of the safety factor from Table I. Since the value for μ_{dp} can vary during lifetime of the brake system, Fig. 4 depicts the clamping forces for the researched adhesion coefficients as grey box. Further, different combinations of brake disc diameters (D) and brake pad widths (B), that are related to series SUV applications of the same manufacturer, are considered. For the following sizing the second combination is used, since it equals the original brake setup of the target vehicle.

An essential part of by-wire systems is the electric motor. From the project, additional specifications must be considered: the actuator has to be driven by 48 VDC, the maximum, electrical power shall not exceed 1.5 kW per corner and must be realized as dual-motor layout due to redundancy reasons. In case of electric motors with high speed range, the maximum torque is quite low and vice versa. On the other hand, high-torque electric motors consume more power and have bigger dimensions. In case of a high speed range, a reducer with high ratio is necessary, which might affect the size negatively. Research on brushless motors with small size lead to mobile robot applications, where a suitable motor was found with the specifications in Table 2.

To translate the rotary into a linear motion of the brake pad carrier in order to generate the clamping force, a transmission device is needed. Different approaches were outlined in the survey [19], showing that most concepts on the market use a combination of (planetary gear) reducer and a (ball) screw drive to amplify the motor torque. Since the electric motor comes with an integrated planetary gear reducer with a ratio of 64:1 already, the use of conventional transmissions will decrease the nominal speed too much, so regulatory requirements (e.g., for maximum brake application time) wouldn't be fulfilled any longer. Further, when using two motors, there are strict requirements for linear guidance of the brake pad carrier or the caliper might lock in case of failure of one motor. Hence, the concept uses a planar cam drive. This transmission is characterized by periodic output motion and in the present case, both sides can be moved independently. In addition, it is possible to realize the gear with small size. Feasibility of the cam design was recently showcased in the research carried out by Yan et al. [53]. The basic mechanism in the actual concept is based on a design by Vienna Engineering (see [54]), but adapted to the actual requirements of a dual-motor brake caliper. A scheme with the acting forces is shown in Fig. 5. As shown there, the design uses eccentricities to move the brake pad carrier. The ratio of the lever amplifies the motor torque at very small space. Reformulating the equilibrium of the electric motor torque (T_m), load torque (T_{lo}), generated by the clamping force and the eccentricity between motor shaft and force action point (e_m), and consideration of friction in the system (T_{fr}), the minimum ratio of levers (l_1/l_2) is given by eq. (9), where i_m is the total number of motors, and η_{tr} is the transmission efficiency, respectively. It is important that the ratio is not set too high, as this increases the application dynamics. A standard, median brake application time is t_{app} = 0.2 s. With the nominal motor speed (n_m) from Table 1, the maximum displacement angle (φ_{max}) is given by eq. (10).

$$\frac{l_1}{l_2} \geq \frac{F_{cl} e_m + T_{fr}}{i_m T_m \eta_{tr}} \tag{9}$$

$$\varphi_{max} \leq \frac{2\pi n_m}{60} \frac{l_2}{l_1} t_{app} \tag{10}$$

TABLE 1 Technical data of the target vehicle

Parameter	Symbol	Unit	Value
Vehicle total mass	m_v	[kg]	2800
Rear load ratio	ψ	[1]	0.51
Normalized height of COG	χ	[1]	0.205
Target braking intensity	z_{trg}	[%]	70
Pad-disc friction coefficient	μ_{dp}	[1]	0.43
Dynamic tire radius	r_{dyn}	[mm]	378
Safety factor	s_F	[1]	1.2

TABLE 2 Technical data of electric motor CubeMars AK80-64 (see [52])

Parameter	Symbol	Unit	Value
Input voltage	$V_{m,in}$	[V]	48
Output torque (nominal / peak)	T_m	[Nm]	48 / 120
Output power (nominal / peak)	P_m	[W]	340 / 900
Motor speed (nominal / peak)	n_m	[rpm]	23 / 48
Motor inertia	I_m	[kg·m²]	5.64×10^{-5}
Total Mass	m_m	[kg]	0.85

The effective pad height and air gap result in a maximum application distance (s_{max}) of 6.5 millimeters, so eq. (11) gives the length l_1.

$$l_1 \leq \sqrt{\frac{{s_{max}}^2}{4\sin\left(\frac{\varphi_{max}}{2}\right) - \sin^2\left(\varphi_{max}\right)}} \tag{11}$$

Referring to Fig. 5, the ratio of F_m/F_{cl} depends on the actuation angle. The closer lever l_2 comes to the position, at which it is parallel to the brake disc, the higher the transmission. By reaching the apex, self-amplification takes place, as the rotating brake disc forces the brake pad into contact. This could cause wheel lock, if the maximum motor torque is not high enough to counteract. Therefore, a stopping pin is integrated, see Fig. 5, that holds the brake pad carrier at a defined position

FIGURE 5 Scheme of the actuation principle with electric motor (①), actuation disc (②), lever (③), brake pad on the brake pad carrier (④), stopping pin (⑤), and brake disc (⑥)

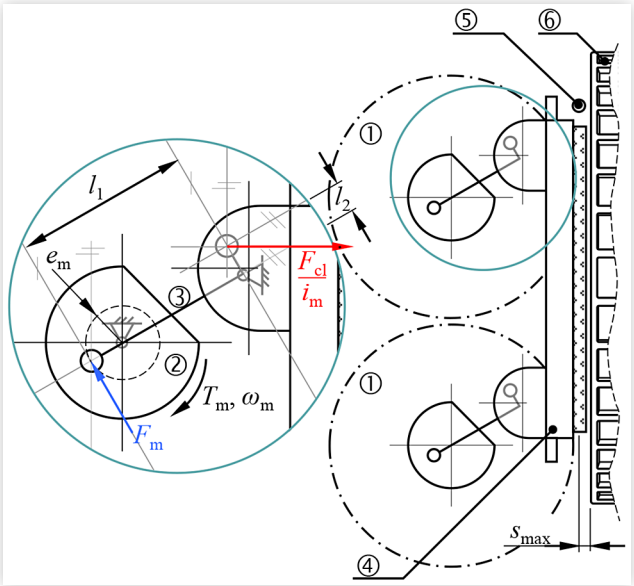

Design of the Power Electronics Components

A DC/DC converter is required to transform the 400 VDC from the traction battery to 48 VDC for the motor. This equals a winding ratio between the primary and secondary side of 1:8. Due to its capability for high switching frequencies and high efficiency, see [55], a LLC resonant converter is used (see Table 3 and Fig. 6).

For design validation, a simulation with static load was carried out on the power electronics in the software PLECS as shown in Fig. 7. The load changes at t = 0.2 seconds, leading to an increased output power (P_{out}). Due to that, the electrical output current (I_{out}) rises and falls back to approximately 14 A in less than 0.01 s. This behavior is due to the used setup: The simulated load owns no dynamics as a normal electric motor, that can be simplified with an internal resistance and capacity. Therefore, the signal can perform a step in simulation, but this will not happen in reality. However, the plot depicts, that the converter is able to restore the voltage output (V_{meas}) to the reference value of V_{ref} = 48 VDC rather quick and to maintain it.

Additionally, further simulations at different loads were performed. From the data, the total power losses and further the efficiency were determined, see Fig. 8. From the virtual assessment, a maximum efficiency ratio of > 98 % was determined. Similar to the first converter, a second unit was developed as part of the safety concept, which is described next. The general structure of the converter is similar to the first one, so no further description is given here.

TABLE 3 Technical data of the target LLC converter

Parameter	Symbol	Unit	Value
Magnetizing inductance	L_{mag}	[µH]	385
Resonant inductance	L_{res}	[µH]	55
Resonant capacity	C_{res}	[nF]	46

FIGURE 6 3D model of the converter with (1) power switches, (2) resonant tank, (3) transformer, (4) diode rectifier with filter and (5) driver unit.

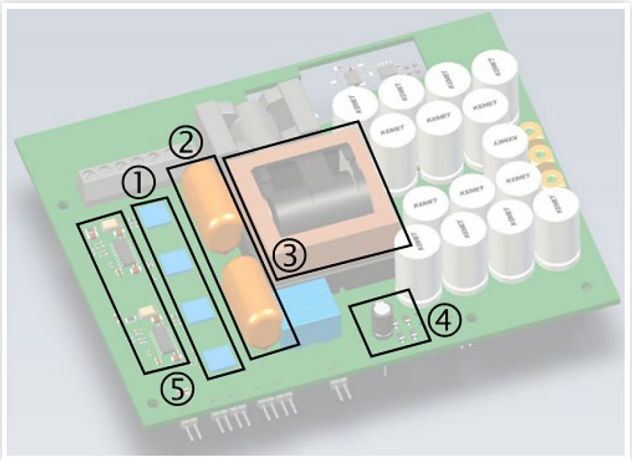

FIGURE 7 Results of converter performance for one simulation loop of t = 0.8 s

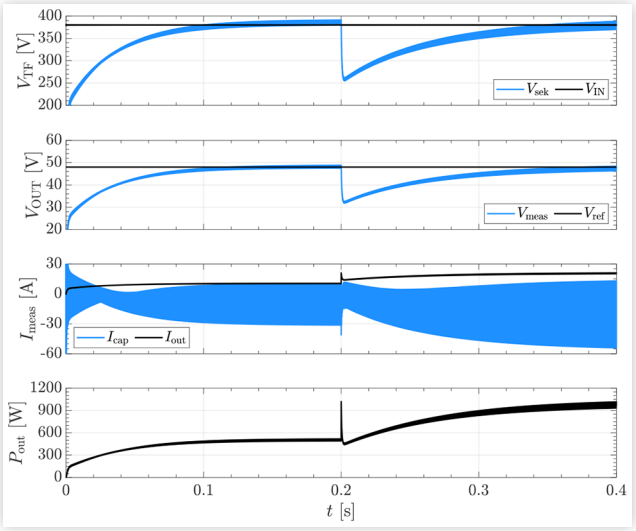

FIGURE 8 Results for investigations on the converter efficiency

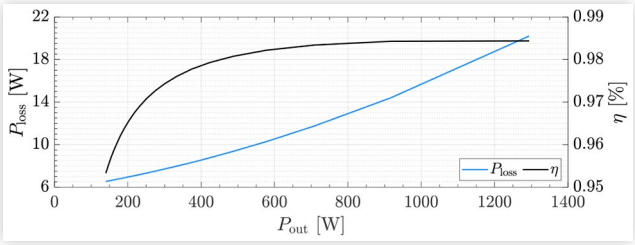

Functional Safety Concept

Safety is defined as the "absence of unreasonable risk" and *functional safety* as "specification of the functional safety requirements, with associated information, their allocation to elements within the architecture, and their interaction necessary to achieve the safety goals" ([1], Part 1). In the vehicle sector, these measures are defined by the *Automotive Safety Integrity Levels* (*ASILs*), see [1], Part 12. Basically, the ASILs are derived from a *Hazard Analysis and Risk Assessment*, where any failure's features *exposure*, *controllability*, and *severity* are rated. The sum of all three defines the ASIL. As an example: Loosing one backlight is not unlikely, but well controllable and without harm, so the ASIL is very low. In contrast, the loss of the brake system can lead to severe harm or even death. Hence, a brake system receives the highest classification, which is ASIL D. This means any failure with very high exposure (E4), lethal end (S4) and uncontrollability (C3) must not occur 10^{-7}/h, which equals once per 10^4 years. To guarantee this, the proposed system has to be fail-operational, so redundancy concepts (e.g., double wiring, second energy storage) are needed for the case of spontaneous power loss.

One crucial failure in brake-by-wire systems is the loss of the supply with electric energy, which leads directly to a failure of the actuators. Figure 9 shows a scheme of the concept for the present brake-by-wire system. In particular, three power supplies are integrated. First is the 400 VDC system from the traction battery, mainly used for driving and storage of regenerated energy. Second is the 12 VDC (lead-acid) battery, which supplies auxiliaries with low power demand. Finally, a 48 VDC battery for the supply of the brake system, is additionally installed. Even, that many modern BEVs do not have a 48 VDC battery, since it was primarily used in mild-hybrid electric vehicles, it seems likely to integrate it, since new x-by-wire chassis systems have higher power demands, that are no longer compatible to the 12 VDC board net solely. Besides the storages, one bi- (⇔) and two unidirectional (⇨) DC/DC converters are used. Further, every storage owns a battery management system (BMS) for optimal power balancing and state observation. These components are not discussed in this paper, since there are mature parts already available. In addition, there won't be any further explanation of the rear axle. As already stated, this article is focused on the front calipers, since EMB for rear axle applications do already have an adequate maturity and can be supplied by the 12 VDC board net. However, they are not taken into account in the safety concept, but are shown in Fig. 9 for the sake of completeness. In the next sections, several failure scenarios are discussed to better explain the strategies for making the system fail-operational. These use cases (UCs) are intended as examples, even if the likelihood during use of the vehicle is low.

UC 1: The first use case under investigation is any event, that leads to a complete failure of the 400 VDC-to-48 VDC converter as the main supply for the brake-by-wire-system. In this case, the electric energy for brake actuation comes from an integrated 48 V lithium-ion battery. In case, there is no power demand from the brake system, a second DC/DC converter recharges the battery from the 12 VDC board net.

UC 2: Second use case describes complete failure of the 48 VDC battery. As with UC 1, the electric energy then

FIGURE 9 Brake system and redundant power supply layout

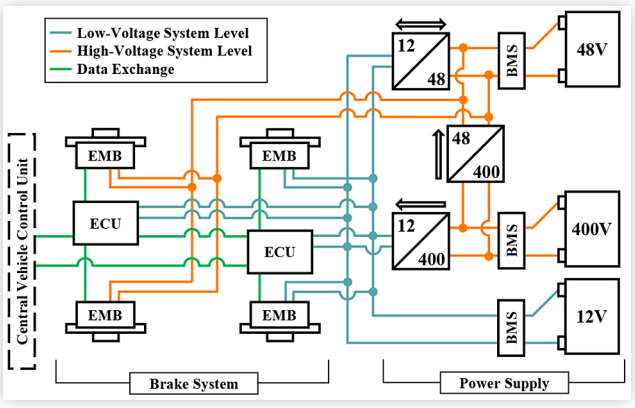

comes directly from the traction battery through the main DC/DC converter.

UC 3: Similar to the first use case, the main supply gets cut-off through any failure of the traction battery. The power supply is then shifted to the 48 VDC battery, but since a loss of the traction battery leads to complete loss of traction power too, only braking to standstill and activation of the parking brake needs to be supported.

UC 4: Besides the high-voltage components, a loss of the 12 VDC board net can be crucial, since the control units and EMB calipers on the rear axle are supplied with low-voltage. Therefore, this case needs to be investigated too. In case of losing the 12 VDC supply, the electric energy can be taken from the bidirectional converter, which is connected to the 48 VDC battery.

UC 5: Since digitalization and driving automation is evolving, the software must be considered too. This means cross-checks, whether the signals from the calipers are logical and equal to the demands coming from the control unit(s). If not, a safety mechanism needs to be installed, that compares the signals constantly and suppresses any command to a faulty caliper. This excludes a shut-down of the whole brake system.

Future Research Ambitions

In the previous sections, a concept for pure EMB system, suitable for BEVs, was introduced. Unlike other approaches, the current design does not use spindle drives, but a planar cam transmission in addition with a dual-motor design for functional safety aspects. Further, the power electronics were designed and simulated. Despite these achievements, some further aspects shall be mentioned. These points are carried out in future research.

First, the system's packaging has to be optimized. With choice of a high-torque motor, a system for mobile robot applications was found. This motor comes with an integrated planetary gear reducer, that provides a good torque density, but increases its size to nearly 10 cm in diameter. Since two of these motors are required for redundancy reasons, it is quite challenging to apply both on existing floating brake calipers. Moreover, both together have a mass of approximately 1.7 kilograms, increasing the unsprung masses of the vehicle and leading to lower eigenfrequencies of the corner, what is negatively affecting the ride comfort. Further research on more compact motors is mandatory. In the opinion of the authors, these motors need to be developed in strong collaboration with clients, since the systems available on the market do not fit every application.

For the simulations, the system was splitted into mechanics and power electronics due to the different development stages of the components. The simulations on the power electronics were performed with static loads, which just gives a limited outcome of the real performance. Since it is possible to simulate both parts in Simulink, a combined simulation would be a) more reliable and b) useful for other investigation e.g., vehicle dynamics and motion control. Further, the system works without any active safety or stabilization control at the moment. For evaluation of braking performance and braking stability, the future implementation of standard systems like antilock braking system and electronic stability control should be considered.

Conclusion

This paper discusses a possible conception of a full EMB system for front axle applications on BEVs, since electromechanical calipers for the rear axle are already available with adequate maturity. The design uses a planar cam drive in combination with an angular lever instead of spindle or ball screw drive. With this approach, it was possible to design a transmission in a dual-motor EMB actuator, that is less space consuming. Additionally, two DC/DC converters has been designed to enable the brake system to be supplied directly from the 400 VDC traction battery and the 12 VDC board net as well to establish a fail-operational system layout for proper performance and low risk even in case of loss of electric power. During the virtual functionality verification tests, the used converters proofed their feasibility to provide a stable power supply at 48 VDC and both achieved a component efficiency ratio of over 98 %. Further, a safety concept was discussed for specific use cases.

After design and virtual development, a physical prototype will be built for experiments under real conditions and for durability tests as well as penetration tests to verify the safety concept. Currently, the system is still in design stage, but it is expected by the authors to have a first prototype by middle of the year.

References

1. International Organization for Standardization (ISO), "Road vehicles – Functional Safety," *ISO 26262* (2018).
2. Economic Commission for Europe, "ECE-R13H: Uniform Provision Concerning the Approval of Vehicles of Categories M, N and O with Regard to Braking," 2015.
3. Li, T. et al., "Research on Mechanism and Key Technology of Intelligent Vehicles Brake By Wire system," in *3rd Conference on Vehicle Control and Intelligence (CVCI)*, 2019. doi:10.1109/CVCI47823.2019.8951547.
4. Gong, X. et al., "Review on the Development, Control Method and Application Prospect of Brake-by-Wire Actuator," *Actuators* 9, no. 1 (2020): 15-38, doi:10.3390/act9010015.
5. Meng, B. et al., "A Survey of Brake-by-Wire System for Intelligent Connected Electric Vehicles," *IEEE Access* 8 (2020): 225424-225436, doi:10.1109/ACCESS.2020.3040184.
6. Li, D. et al., "Review of Brake-by-Wire System and Control Technology," *Actuators* 11, no. 3 (2022): 80-96, doi:10.3390/act11030080.

7. Zhang, L. et al., "Brake-By-Wire System for Passenger Cars: A Review of Structure, Control, Key Technologies, and Application in X-By-Wire Chassis," *eTransportation* 18 (2023): 100292-100306, doi:10.1016/j.etran.2023.100292.
8. Hua, X. et al., "A Review of Automobile Brake-by-Wire Control Technology Processes," *Processes* 11, no. 4 (2023): 994-1013, doi:10.3390/pr11040994.
9. Gombert, B. and Gutenberg, P., "Die elektronische Keilbremse. Meilenstein auf dem Weg zum elektrischen Radantrieb," *Automobiltechnische Zeitschrift (ATZ)* 108, no. 11 (2006): 904-913, doi:10.1007/BF03221829.
10. Ho, L. et al., "The Electronic Wedge Brake – EWB," SAE Technical Paper 2006-01-3196 (2006), doi:10.4271/2006-01-3196.
11. Yu, L. et al., "Magnetorheological and Wedge Mechanism-Based Brake-by-Wire System With Self-Energizing and Self-Powered Capability by Brake Energy Harvesting," *IEEE/ASME Transactions on Mechatronics* 21, no. 5 (2016): 2568-2580, doi:10.1109/TMECH.2015.2512579.
12. Hasan, M.H.C. et al., "Modelling and Design of Optimized Electronic Wedge Brake," in *IEEE International Conference on Automatic Control and Intelligent Systems (I2CACIS)*, 2019. doi:10.1109/I2CACIS.2019.8825045.
13. Ahmad, F. et al., "Modelling and Control of a Fixed Calliper-Based Electronic Wedge Brake," *Journal of Mechanical Engineering* 63, no. 7 (2018): 181-190, doi:10.5545/sv-jme.2016.3508.
14. Ahmad, F. et al., "Simulation and Experimental Investigation of Vehicle Braking System Employed a Fixed Caliper Based Electronic Wedge Brake," *Simulation: Transactions for the Society for Modeling and Simulation International* 94, no. 4 (2018): 327-340, doi:10.1177/0037549717733805.
15. Xu, F. and Cho, C., "A Novel Electronic Wedge Brake Based on Active Disturbance Rejection Control," *Energies* 15, no. 14 (2022): 5096-5113, doi:10.3390/en15145096.
16. Xue, X., Cheng, K.W.E., and Fan, Y., "Topology and Analysis of An Electromechanical Brake for Electric Vehicles," in *8th International Conference on Power Electronics Systems and Applications (PESA)*, 2020. doi:10.1109/PESA50370.2020.9343958.
17. Xiao, F. et al., "Design and Control of New Brake-by-Wire Actuator for Vehicle Based on Linear Motor and Lever Mechanism," *IEEE Access* 9 (2021): 95832-95842, doi:10.1109/ACCESS.2021.3094030.
18. Baek, S.-K. et al., "Evaluation of Efficient Operation for Electromechanical Brake Using Maximum Torque per Ampere Control," *Energies* 12, no. 19 (2019): 1869-1181, doi:10.3390/en12101869.
19. Yan, Z. et al., "Design, Modeling, and Control of Electronic Mechanical Brake System: A Review," *SAE Int. J. Veh. Dyn., Stab., and NVH* 8, no. 4 (2024): 2024, doi:10.4271/10-08-04-0026.
20. Li, Y. et al., "Control System Design for Electromechanical Brake System Using Novel Clamping Force Model and Estimator," *IEEE Transactions on Vehicular Technology* 70, no. 9 (2021): 8653-8668, doi:10.1109/TVT.2021.3095900.
21. Xu, Z. and Gerada, C., "Enhanced Force Estimation for Electromechanical Brake Actuators in Transportation Vehicles," *IEEE Transactions on Power Electronics* 36, no. 12 (2021): 14329-14339, doi:10.1109/TPEL.2021.3085996.
22. Chu, L., Zhu, P., and Chang, C., "Research on Full Brake-By-Wire System and Clamping Force Estimation Strategy Based on Redundant Drive Motors," *IEEE Access* 11 (2023): 124098-124113, doi:10.1109/ACCESS.2023.3330215.
23. Wei, W., He, T., and Pal, A., "Real-time Clamping Force Estimation of Brake-by-Wire System for Electric Autonomous Vehicles," *American Control Conference (ACC)* (2023), doi:10.23919/ACC55779.2023.10156643.
24. Jo, C., Hwang, S., and Kim, H., "Clamping-Force Control for Electromechanical Brake," *IEEE Transactions on Vehicular Technology* 59, no. 7 (2010): 3205-3212, doi:10.1109/TVT.2010.2043696.
25. Li, T. et al., "Clamping Force Control Strategy of Electromechanical Brake System," in *4th International Conference on Mechanical Engineering, Intelligent Manufacturing, and Automation Technology (MEMAT)*, 2023. doi:10.3390/act12070272.
26. Zhao, Y., Lin, H., and Li, B., "Sliding-Mode Clamping Force Control of Electromechanical Brake System Based on Enhanced Reaching Law," *IEEE Access* 9 (2021): 19506-19515, doi:10.1109/ACCESS.2021.3052944.
27. Lee, C.F. and Manzie, C., "High-Bandwidth Clamp Force Control for an Electromechanical Brake," *SAE Int. J. Pass. Cars - Electron. Electr. Syst.* 5, no. 2 (2012): 590-599, doi:10.4271/2012-01-1799.
28. Kim, C. et al., "An Application of the Brain Limbic System-Based Control to the Electromechanical Brake System," *Advances in Mechanical Engineering* 10, no. 2 (2018), doi:10.1177/1687814018755215.
29. Chen, S., Zhang, X., and Wang, J., "Sliding Mode Control of Vehicle Equipped with Brake-by-Wire System considering Braking Comfort," *IEEE Access* 9 (2021): 19506-19515, doi:10.1155/2020/5602917.
30. Haggag, S.A. and Abidou, D., "An Approach to Vehicle Brake-By-Wire Optimal Control Tracking Strategy," *SAE Int. J. Pass. Cars - Mechanical Systems* 6, no. 1 (2013): 154-162, doi:10.4271/2013-01-0686.
31. Riva, G. et al., "Robust Force Control for Brake-By-Wire Actuators via Scenario Optimization," *IFAC-PapersOnLine* 53, no. 2 (2020): 1-6, doi:10.1016/j.ifacol.2020.12.025.
32. Li, J. et al., "A design of electromechanical brake system triple-loop controllers using frequency domain method based on Bode plot," in *International Conference on Transportation, Mechanical, and Electrical Engineering (TMEE)*, 2011. doi:10.1109/TMEE.2011.6199322.
33. Juneid, M.S., Zöldy, M., and Harth, P., "Sensorless Optimal Control of Electronic Wedge Brake based on Dynamic Model and Kalman Filter State Multiple-Estimation," *Proceedings of the Institution of Mechanical Engineers, Part D: Journal of Automobile Engineering* 238, no. 9 (2024): 2802-2816, doi:10.1177/09544070231168168.
34. Li, Y. et al., "Effective Clamping Force Control for Electromechanical Brake System," *IEEE/ASME*

International Conference on Advanced Intelligent Mechatronics (AIM) (2020), doi:10.1109/AIM43001.2020.9158796.

35. Chen, Q. et al., "Clamping Force Control Strategy of Electro-Mechanical Brake System Using VUF-PID Controller," *Actuators* 12, no. 7 (2023): 272-283, doi:10.3390/act12070272.
36. Xu, Z., "An Adaptive Clamping Force Control Strategy for Electro-Mechanical Brake System Considering Nonlinear Friction Resistance," SAE Technical Paper, 2024-01-2282 (2024), doi:10.4271/2024-01-2282.
37. Cheon, J. et al., "Brake By Wire Functional Safety Concept Design for ISO/DIS 26262," SAE Technical Paper 2011-01-2357 (2011), doi:10.4271/2011-01-2357.
38. Jeon, K. et al., "Electronic Brake Safety Index for Evaluating Fail-Safe Control of Brake-By-Wire Systems for Improvement in the Straight Braking Stability," *Proceedings of the Institution of Mechanical Engineers, Part D: Journal of Automobile Engineering* 228, no. 8 (2014): 873-893, doi:10.1177/0954407014522032.
39. Stolte, T., "Ensuring Functional Safety by Networking Systems from Different Domains, Illustrated by the Example of an Electromechanical Brake," in *5th International Munich Chassis Symposium*, 2014. 10.1007/978-3-658-05978-1_41.
40. Leu, K.-L. et al., "An Intelligent Brake-By-Wire System Design and Analysis in Accordance with ISO-26262 Functional Safety Standard," in *International Conference on Connected Vehicles and Expo (ICCVE)*, 2015. doi:10.1109/ICCVE.2015.20.
41. Putz, M.H. and Zipper, T., "Functional Safety (ASIL-D) for an Electro Mechanical Brake," SAE Technical Paper 2017-01-2517 (2017), doi:10.4271/2016-01-1953.
42. Schlimme, H.C. and Henze, R., "Brake-by-Wire System Redundancy Concept for the Double Point of Failure Scenario," *SAE Int. J. Veh. Dyn., Stab., and NVH* 7, no. 3 (2023): 329-341, doi:10.4271/10-07-03-0021.
43. Schrade, S. et al., "Safety Concepts for Future Electromechanical Brake Actuators," *SAE Int. J. Passeng. Veh. Syst.* 17, no. 3 (2024), doi:10.4271/15-17-03-0012.
44. Breuer, B. and Bill, K.H., *Brake Technology Handbook* (SAE International, 2008)
45. Pacejka, H.B., *Tire and Vehicle Dynamics*, 3rd ed. (Butterworth-Heinemann, 2012)
46. Kchaou, M. et al., "Friction Characteristics of a Brake Friction Material under Different Braking Conditions," *Materials & Design* 1980-2015, no. 52 (2013): 533-540, doi:10.1016/j.matdes.2013.05.015.
47. Orlowicz, A.W. et al., "Coefficient of Friction of a Brake Disc-Brake Pad Friction Couple," *Archives of Foundry Engineering* 16, no. 4 (2016): 196-200, doi:10.1515/afe-2016-0109.
48. Kumar, N. et al., "The Evolution of Brake Friction Materials: A Review," *Materials Physics and Mechanics* 47 (2021): 796-815, doi:10.18149/MPM.4752021_13.
49. Hamatschek, C. et al., "Comparative Study on the Friction Behaviour and the Particle Formation Process between a Laser Cladded Brake Disc and a Conventional Grey Cast Iron Disc," *Metals* 13, no. 2 (2023): 300-318, doi:10.3390/met13020300.
50. Liew, K.W. and Nirmal, U., "Frictional Performance Evaluation of Newly Designed Brake Pad Materials," *Materials & Design* 48 (2013): 25-33, doi:10.1016/j.matdes.2012.07.055.
51. Bashor, M., Saleem, S.S., and Bashir, O., "Friction and Wear Behaviour of Disc Brake Pad Material using Banana Peel Powder," *International Journal of Research in Engineering and Technology* 4, no. 2 (2015): 650-659, doi:10.15623/IJRET.2015.0402091.
52. Mars C. (Ed.), "AK80-64," [Online]. Available: https://www.cubemars.com/goods-1143-AK80-64.html.
53. Yan, Z. et al., "Design and Optimization of a Novel Electronic Mechanical Brake Actuator Based on Cam," *Actuators* 12, no. 8 (2023): 329-351, doi:10.3390/act12080329.
54. Putz M., U.S. Patent 9970498B2, 2015-05-05, "Electrically Actuated Friction Brake," [Online], Available: Google Patents.
55. Pan, H. et al., "Pulse-Width Modulation Control Strategy for High Efficiency LLC Resonant Converter with Light Load Applications," *IET Power Electronics* 7, no. 11 (2014): 2887-2894, doi:10.1049/iet-pel.2013.0846.

Contact Information

Marius Heydrich, Matthias Lenz, and Valentin Ivanov
Technische Universität Ilmenau
marius.heydrich@tu-ilmenau.de, matthias.lenz@tu-ilmenau.de, valentin.ivanov@tu-ilmenau.de

Julian Stoev, Johan Lecoutere
Bluways International BVBA
julian.stoev@bluways.com, johan.lecoutere@bluways.com

Acknowledgement

The research leading to these results was funded by the European Union under the Horizon 2020 Research and Innovation Programme under Grant Agreement No. 101056824 (HighScape). Views and opinions expressed are however those of the author(s) only and do not necessarily reflect those of the European Union or the European Climate, Infrastructure and Environment Executive Agency (CINEA). Neither the European Union nor CINEA can be held responsible for them.

Definitions, Acronyms, Abbreviations

ASIL - Automotive Safety Integrity Level
BBW - Brake-by-Wire
BEV - Battery Electric Vehicle
COG - Center of Gravity
DC - Direct Current
ECU - Electronic Control Unit
EMB - Electromechanical brake
SUV - Sport Utility Vehicle
UC - Use Case

ISSN 0148-7191